It should be noted that from the technological point of view it is easier to obtain zirconium-containing ceramics. Its sintering range is 80°C and the optimum firing temperature is 1300 ± 40°C.

The investigations show that the process of cordierite formation is the material, based on finely dispersed glass powders of almost cordierite composition and a clay component, proceeds in the field of low temperatures (900-1000°C). In this process the cordierite formation takes place through a metastable quartzlike phase which is characteristic only of the crystallization of glasses of similar compositions.

It has been established that the addition of ZrO_2 helps to expand the temperature range of sintering. The major action of zirconium dioxide affects the early stages of firing (900-1000°C). In this temperature interval the shrinkage of the material is 7% and its open porosity does not exceed 10%. The presence of zirconium dioxide in the glass composition, on one hand, helps to increase the centers of crystallization, and on the other, due to the higher viscosity of zirconium-containing glasses, their growth is maintained. Therefore, the material with ZrO_2 addition is characterized by somewhat larger amount of residual glass phase at low temperatures. This ensures more complete sintering in the range of these temperatures and widening of the sintering interval of this material.

As a result of the above study, a densely sintered cordierite ceramic material has been obtained with wide range of sintering and optimum firing temperature of 1300 ± 40°C. The obtained material possesses better physicotechnical properties and is recommended for making wares by semidry and plastic shaping.

LITERATURE CITED

1. V. G. Avetikov and É. I. Zin'ko, Magnesian Electroceramics [in Russian], Énergiya, Moscow (1973).
2. E. A. Takher, É. P. Dain, T. I. Fedoseeva, and G. S. Lenskaya, Steklo Keram., No. 11 (1973).
3. E. A. Takher, T. I. Fedoseeva, V. Yu. Kellerman, and R. Ya. Popil'skii, Steklo Keram., No. 2 (1974).
4. E. Gerasimova and L. Lepkova, Stroit. Mater. Silik. Prom., No. 8 (1972).
5. I. D. Tykachinskii, in: Study of Glass-Forming Systems and Synthesis of New Glasses Based on Them [in Russian], VNIIÉSM, Moscow (1971).
6. S. M. Oheberg and D. W. Strickler, J. Am. Ceram. Soc., 45, No. 4 (1962).

INVESTIGATION OF DEFORMATION PROPERTIES OF SILICON-CARBIDE-CONTAINING MATERIALS

G. A. Gogotsi, Ya. L. Grushevskii, N. N. Radin, V. G. Panteleev, and K. S. Ramm

UDC 666.765:539.4

The problem of agreement between calculated values for the criteria of thermal stability determined on the basis of the properties of the materials and the results of their experimental evaluation is closely related to the need for reliable determination of the physicomechanical properties which enter into these criteria. Bend tests are most often used to study the strength of brittle heat-resistant materials. The data obtained is treated according to equations based on hypotheses of elasticity theory. The results obtained in this fashion can be considered for the majority of industrial refractory materials only as approximate in view of the fact that their true stress– strain curves are not linear in most cases.

Silicon-carbide-containing materials [1] do not deform elastically. The present work is a study of these materials.

The materials were tested in pure bending on a modern tensile machine RM-101M [2] permitting sufficient accuracy to determine the stress in the 0-100 kg range. The samples from the silicon-carbide-containing

Institute of Strength Problems, Academy of Sciences of the Ukrainian SSR. State Ceramics Research Institute.

Translated from Steklo i Keramika, No. 10, pp. 27-29, October, 1976.

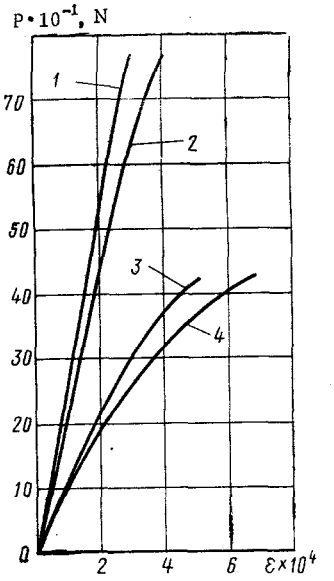

Fig. 1

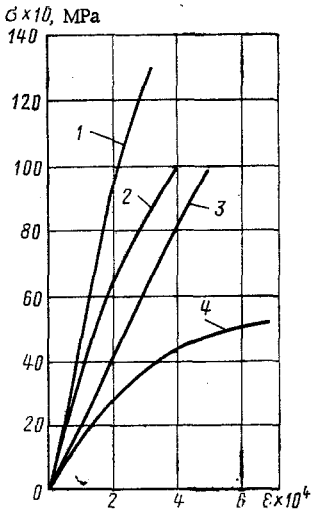

Fig. 2

Fig. 1. Load–deformation curves: 1) M-2 composition in compression; 2) the same in tension; 3) M-3 composition in compression; 4) the same in tension.

Fig. 2. Deformation curves: 1) M-3 composition in compression; 2) the same in tension; 3) composition M-2 in compression; 4) the same in tension.

materials (Table 1) were made in the form of prisms with a rectangular cross section 15 × 15 × 120 mm. according to the method described earlier [1].

The magnitudes of the applied stress and deformation were fixed by two-coordinate self-recording apparatuses PDS-021. Deformation was measured by strain gauges of the 2PKP-10-200GB type, which were placed on the specimen in the extension and compression zones. During testing, the stress–strain curves were recorded in coordinates $P = f(\varepsilon)$ for all the materials studied. The rate of approach of the loading supports was 0.1 mm/min, chosen so that the tests would approximate the experiments to determine thermostability properties.

All investigated materials, as noted from the stress–strain curves obtained during testing, deformed nonlinearly and differently during tension and compression. In Fig. 1 the load–deformation curves are shown for tension and compression of several characteristic materials. For the construction of the stress–strain curves, the relationships which take into account the noted peculiarities of the behavior of the materials [2] under load were used as follows:

TABLE 1

Material	Composition of silicon-carbide-containing heat-resistant material, %				Density, g/cm³	Porosity A, %
	silicon carbide	corundum	clay	alumina		
M-1	40	10	30	20	2,45	23.2
M-2	45	25	20	10	2,63	19.3
M-3	70	0	20	10	2,53	18.0
M-4	50	10	30	10	2,52	18.9
M-5	43	17	25	15	2,53	21.5
M-6	58	12	20	10	2,61	18.8
M-7	60	5	25	10	2,51	18.3
M-8	55	5	25	15	2,50	19.8
M-9	45	10	30	15	2,46	21.4
M-10	48	17	25	10	2,52	20.4
M-11	50	10	25	15	2,48	21.4
M-12	52	12	23	13	2,53	20,2

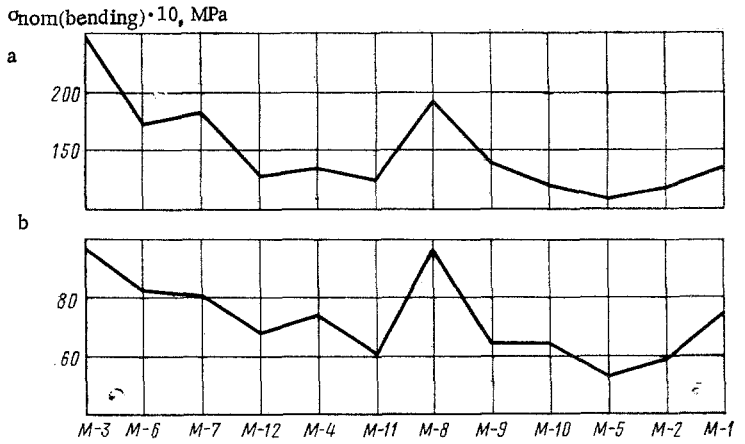

Fig. 3. Comparison of the strength determination results of heat-resistant materials in three-point (a) and four-point (b) bending.

$$\sigma_+ = \frac{a}{bh^2}\left(P + \frac{\varepsilon_{av}}{2}\cdot\frac{dP}{d\varepsilon_{av}}\right)\left(1 + \frac{\varepsilon'_-}{\varepsilon'_+}\right), \tag{1}$$

$$\sigma_- = \frac{a}{bh^2}\left(P + \frac{\varepsilon_{av}}{2}\cdot\frac{dP}{d\varepsilon_{av}}\right)\left(1 + \frac{\varepsilon'_+}{\varepsilon'_-}\right). \tag{2}$$

where σ_+ and σ_- are the stresses acting in tensile and compressive surface layers of the sample; a is the distance between the outside and inside loading members; b is the width; h is the thickness of the sample; P is the applied force; ε_+ and ε_- are the deformations of the layers;

$$\varepsilon'_+ = \frac{d\varepsilon_+}{dP};\quad \varepsilon'_- = \frac{d\varepsilon}{dP};$$

$$\varepsilon_{av} = (\varepsilon_+ + \varepsilon_-)/2.$$

Constructing the deformation curves of the materials according to Eqs. (1) and (2) one can determine the true strength in bending, $\sigma_{fr\,(bending)}$ as the largest stress value on the $\sigma_+ - \varepsilon_+$ curve.

The elastic modulus in tension is calculated according to the equation

$$E_+ = \frac{3a}{bh^2}\cdot\frac{\varepsilon'_-}{(\varepsilon'_+)^2}, \tag{3}$$

where the derivatives are determined when the force is equal to zero.

The measure of brittleness [2] characterizing the nonelasticity of the materials, their deformation characteristics, and their fracture, is determined by the expression

$$\chi = \frac{\sigma^2_{fr\,(bending)}}{2E_+\int_0^{\varepsilon_{ult}}\sigma_+ d\varepsilon_+} \tag{4}$$

where ε_{ult} is the ultimate tensile deformation.

TABLE 2

Material	$\sigma_{fr\,(bending)}$·10, MPa	$E_{sec}\cdot 10^{-4}$, MPa	$\sigma_{nom\,(bending)}$·10, MPa	$E_+\cdot 10^{-4}$, MPa	$\sigma_{av\,(bending)}$·10, MPa	$E_{av}\cdot 10^{-4}$, MPa	$\varepsilon_{ult}\cdot 10^4$ (rel. units)	χ
M-1	92	2,13	74	2,86	81	2,85	4,31	0,48
M-2	81	1,73	58	2,36	68	2,45	4,78	0,37
M-3	128	3,45	97	4,44	110	4,38	3,72	0,68
M-4	91	2,10	74	2,87	80	2,90	4,35	0,50
M-5	84	1,64	53	2,05	69	2,42	5,16	0,29
M-6	103	2,52	83	3,03	91	3,36	4,09	0,53
M-7	124	2,48	81	4,00	101	3,68	5,00	0,24
M-8	115	2,76	98	3,17	106	3,56	4,20	0,62
M-9	84	1,99	64	2,54	73	2,75	4,25	0,48
M-10	74	1,71	65	2,13	61	2,18	4,36	0,58
M-11	92	2,12	60	2,69	78	2,85	4,40	0,32
M-12	92	2,02	68	2,67	79	2,82	4,56	0,39

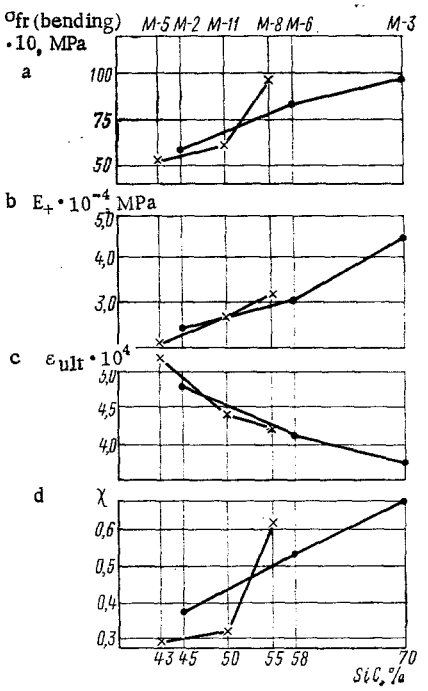

Fig. 4

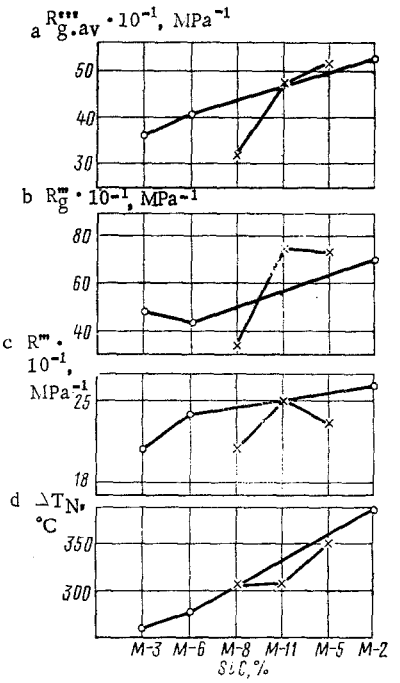

Fig. 5

Fig. 4. The dependence of strength and elastic properties (in bending): a) true strength; b) elastic modulus in tension; c) ultimate tensile deformation; and d) brittleness on the silicon carbide content in heat-resistant materials.

Fig. 5. The dependence of thermostability properties: a) criteria on $R'''_{g.av}$; b) criterion R'''_g; c) criterion R'''; d) temperature drop, measured at the moment of fracture initiation on the silicon carbide content in the heat-resistant material.

The mechanical properties obtained during testing in pure bending are given in Table 2. There for comparison are also shown the average strength values, σ_{av}. and the elastic modulus, E_{av}. for the calculation of which the difference in tensile and compression deformation was not considered, i.e., $\varepsilon_+ = \varepsilon_- = \varepsilon_{av}$; also shown are the nominal strength during bending $\sigma_{nom\,(bending)}$, and the secant modulus, E_s, determined from the equation for the strength of the materials.

From the data in Table 2 it is evident that neglecting the true behavior of a material results in a significant distortion in the values for the strength and elasticity.

To construct the deformation curves from the load–deformation curves, the range of changing stress is broken up into discrete intervals where the initial line is approached by the interpolated polynomial of the

TABLE 3

Composition	$R''' \cdot 10^{-1}$, MPa^{-1}	$R'''_g \cdot 10^{-1}$, MPa^{-1}	$R'''_{g.av} \cdot 10^{-1}$, MPa^{-1}	ΔT_N, °C
M-1	25,5	52,0	43,2	377
M-2	26,3	71,0	52,8	382
M-3	21,0	47,3	36,2	258
M-4	25,4	52,5	45,1	296
M-5	23,2	73,0	50,7	351
M-6	23,8	44,0	40,5	279
M-7	16,0	60,6	36,3	287
M-8	20,9	33,0	31,6	306
M-9	28,0	61,2	51,8	321
M-10	31,1	59,7	58,6	320
M-11	25,0	74,6	46,8	307
M-12	23,8	57,7	45,1	282

Lagrangian quadratic, the derivative of which is taken for the value of $d\varepsilon/dP$. Because the calculated differentiation is not accurate [3], i.e., the inaccuracies of the differentiated curve affect very strongly the value of the derivative, the size of the intervals was chosen to give the most accurate approximation of the derivative. The values obtained in this fashion for the derivative were smoothed which also increased the accuracy of the differentiation and consequently the final results.

Deformation curves of the investigated materials were constructed by the described method. The curves for the M-3 and M-2 compositions are shown as an example in Fig. 2.

A comparison of the results (Fig. 3) of the strength determinations given in Table 2 with data from three-point bending obtained earlier [1] shows that using the pure bending method and the described calculation gives not only additional information about the mechanical properties of the materials, but also defines more accurately the ultimate strengths and elastic moduli and also permits the adjustment of the dependence behavior of these properties upon the compositions of the studied materials.

Curves showing the dependence of the investigated properties on the silicon carbide content in the materials were constructed from the experimental results (Fig. 4). To construct these curves two series of monotypic (according to structure bonds) materials were considered: M-2, M-6, M-3 (20% heat-resistant clay and 10% alumina) and M-5, M-11, M-8 (25% heat-resistant clay and 15% alumina). As evident from Fig. 4, despite the change in the percentage (phase) composition bonds, the ultimate strength and elastic modulus of the materials increase in both cases with an increase in silicon carbide content as the deformation decreases. An increase in the brittleness and, consequently, catastrophic failure, the lowering of the relaxation ability, is the result of such behavior of the materials.

Having available the true strength and elastic properties one can compute the criterion* R_g''', which characterizes the resistance of a material to the thermal cracks and is based on the value of the true elastic energy accumulated in a unit volume of material at the beginning moment of macrofracture of the sample [4].

$$R_g''' = \frac{1}{\sigma_{\text{fr(bending}}\,\varepsilon_{\text{elast limit}}} = \frac{E_+}{\sigma^2_{\text{fr(bending)}}};$$

$$R_{g_{\text{av}}}''' = \frac{E_{\text{av}}}{\sigma^2_{\text{av(bending)}}} \qquad (5)$$

The curves for the mentioned two types of material (Fig. 5) constructed on the data in Table 3 for the criterion of thermal stability and experimental temperature drop measured at the moment of fracture initiation in a hollow cylindrical sample show that good agreement is observed between the calculated criterion, $R_{g.av}'''$ and the characteristic thermal stability, ΔT_N. However, the unambiguous dependence between these values is not followed for all the considered materials. There is a correlation only for materials with one type of bond. When the composition bonds are changed and consequently, the structure of the material also, corrections of the criteria are necessary which take into account structural parameters.

LITERATURE CITED

1. G. A. Gogotsi, Ya. L. Grushevskii, V. P. Panteleev, N. N. Radin, and K. S. Ramm, Probl. Prochn., No. 2 (1975).
2. G. A. Gogotsi, Ya. L. Grushevskii, and A. A. Kurashevskii, Ogneupory, No. 1 (1976).
3. G. A. Gogotsi, Probl. Prochn., No. 10 (1973).
4. I. S. Berezin and N. P. Zhidkov, Calculation Methods [in Russian], Nauka, Moscow (1966).
5. G. A. Gogotsi, V. A. Artemov, Ya. L. Grushevskii, and A. A. Kurashevskii, Probl. Prochn., No. 12 (1975).

* The well-known criterion R''' [D. P. H. Hasselman, J. Am. Ceram. Soc., 52, No. 11 (1969)] for the case of determining properties from bend tests for relatively brittle materials which are charactized by a brittleness measure less than unity is based on "fictitious" values which seem essentially high in comparison with the true elastic energy, expressed as $\sigma_{\text{nom (bending)}}/E_{\text{sec}}$.